

Effect of Wall Roughness and Concentration of Clay on Erosion in the Hole Erosion Test

¹Kissi Benaissa, ¹Parron Vera Miguel Angel, ¹Rubio Cintas Maria Dolores,
²El Bakkali Larbi, ²Khamlichi Abdellatif, ²Bezzazi Mohammed and ³Dubujet Philippe
¹Department of Mechanical and Civil Engineering, Polytechnic High School of Algeciras,
University of Cadiz, Ramon Pujol Avenue, Algeciras 11202, Spain
²Department of Physics, Modeling and Simulation of Mechanical Systems Laboratory,
Faculty of Sciences, University Abdelmalek Essaadi, BP 2121,
M'hannech, 93002, Tetouan, Morocco
³Department of Civil Engineering, Laboratory of Tribology and Dynamics of Systems UMR 5513,
National School of Engineers at Saint-Etienne, 77 Jean Parot Street, Saint-Etienne 42042, France

Abstract: Problem statement: Internal soil erosion is a real threat for hydraulic infrastructures. In its final stage it develops in piping involving the formation and progression of a continuous void inside the soil between the upstream and downstream sides. The hole erosion test was introduced to characterize kinematics of piping in terms of the time left to rupture. Actual modeling approaches of this test are essentially one dimensional. The wall shear stress generated by the flow is assumed to be uniform, so that erosion rate is also uniform along the hole length. Experimental observations show however an irregular profile of the eroded hole. **Approach:** In this study an axisymmetric extension representation of the hole erosion test was performed. The biphasic flow at the origin of surface erosion occurring in the porous soil sample was modeled by means of the renormalization group based $k-\epsilon$ turbulence equations. Fluent software package was used to perform the numerical modeling. **Results:** This had enabled to estimate the wall shear stress which was found to be non uniform along the hole length. Erosion rate was then estimated by using a classical law. Its variations as affected by the applied gradient pressure, fluid density as well as the actual fluid/soil interface roughness were analyzed. In particular, wall roughness and clay concentration were found to increase noticeably the erosion rate. **Conclusion/Recommendations:** Predicting erosion rate at the start of piping formation can be done by the proposed model. Flow features are however very complex in the real HET configuration. In particular, clay concentration does not vary equally along the hole length. The erosion law coefficients are variable. Transport phenomenon of some soils particles that detach is present in the problem. Further investigations including these aspects should be performed in order to render more profoundly the complex physics involved in this experiment.

Key words: Piping, hole erosion test, turbulence, $k-\epsilon$ model, wall roughness

INTRODUCTION

Soil erosion constitutes a major source of problems threatening safety of dams and levees. Soil erosion is a complex phenomenon that starts smoothly and develops at its final stage to huge fluid leakages occurring under the hydraulic infrastructures. Piping is the term used to designate these leakages because of void formation that takes place between the upstream and downstream sides. Piping is known to occur insidiously through the soil under foundations and to cause abrupt collapse of structures. Many dam ruptures have happened throughout the world, some of these events have been reported in reference (Foster *et al.*, 2000). Such

catastrophic accidents can result in human casualties and generate large material losses with dramatic consequences at the social and economic levels.

Internal erosion is a progressive degradation of soils which is induced by the action of a flowing fluid through the porous medium. Many research activities related to the experimental and theoretical characterization of this phenomenon are reported in the literature (Wan and Fell, 2004a; 2004b; Bonelli *et al.*, 2006; Fell *et al.*, 2003; Richards and Reddy, 2010).

Internal erosion is associated with fine particles detachment under the effect of forces generated by the flowing fluid. To classify the different stages associated to this phenomenon of particles

Corresponding Author: Khamlichi Abdellatif, Department of Physics, Modeling and Simulation of Mechanical Systems Laboratory, Faculty of Sciences, University Abdelmalek Essaadi, BP 2121, M'hannech, 93002, Tetouan, Morocco
Tel: +212667795068 Fax: +212539994500

detachment and their transport within the soil, two main mechanisms have been introduced: suffusion and piping. Internal erosion associated to suffusion can also be separated, according to (Foster *et al.*, 2000), into four phases: initiation, filtration, progression and rupture by piping development. Initiation starts when the hydraulic gradient exceeds a threshold value. Filtration is a phase which depends on the soil granular constitution and can be modified by the presence of a filter. The progression is the phase associated to development of internal erosion within the soil material. The rupture by a breach is the next phase occurring inside the soil massif. This ultimate phase is followed by piping. Kinematics of piping is very fast and only few moments can separate its initiation from the complete flow break. To characterize piping kinematics, several experiments were designed to reproduce in laboratory conditions surface erosion mechanisms taking place at the fluid/soil interface. Recently, the Hole Erosion Test (HET) was introduced (Wan and Fell, 2004a). This test proved to be simple, fast and well adapted to perform surface erosion characterization during piping development for all investigated cases.

The HET consists in introducing inside a standard mould a cylindrical sample of soil prepared with a hole that is to be tested against surface erosion. The sample length is $L = 117$ mm. The hole pre-perforated along the longitudinal axis of symmetry of the soil sample has a quasi-cylindrical form with radius $R = 3$ mm. A constant hydraulic head is applied between the tube extremities. Depending on the soil constitution, the inlet hydraulic head:

$$H = \Delta p / \rho g$$

Where:

ρ = The fluid density

g = The constant of gravity, is fixed at a level exceeding the outlet head by 50-1200 mm

Theoretical modeling of the HET test has been performed under some assumptions (Bonelli *et al.*, 2006; Lachouette *et al.*, 2008; Bonelli and Brivois, 2008). These models which are essentially one-dimensional proved to be sufficient in explaining the erosion phenomenology related to piping problem. They yield a comprehensive description of the erosion initiation and kinetics for a given soil. These rudimentary models enable also to evaluate the influence of the hydraulic conditions on the kinetics and to quantify the gain in time left to rupture by operating for example partial drainage of the water reserve.



Fig. 1: Sample tested with the HET; surface erosion produced at the fluid/soil interface

In one-dimensional modeling, the surface erosion law is stated traditionally, (Wan and Fell, 2004b), to be given by:

$$\dot{\epsilon}_{er} = c_{er}(\tau - \tau_s)$$

Where:

$\dot{\epsilon}_{er}$ = The erosion rate which corresponds to the mass loss per unit time and per unit surface area

C_{er} = The surface erosion coefficient which measures the soil erodability

τ = The actual shear stress acting at the wall (assumed to be constant along the whole hole length)

τ_s = The shear erosion threshold limit. The erosion happens only if τ exceeds in absolute value τ_s

By using mass conservation of soil, one could easily arrive at:

$$\dot{R} = \dot{\epsilon}_{er} / \rho_d$$

Where:

ρ_d = The dry density of soil sample

R = The actual radius of the tube (Khamlichi *et al.*, 2009)

This last relation predicts uniform radius along the hole during erosion.

Additional aspects associated to the two-dimensional nature of the HET are present in the problem. Figure 1 presents a sample tested with HET. It shows that the inlet side (bottom) of the hole has undergone much more erosion than the outlet side (top). As seen previously one-dimensional modeling of this test could not predict this eroded shape since it yields uniform erosion at the fluid/soil interface.

Erosion can be affected also by roughness of the hole wall. In many other engineering problems roughness was recognized to have crucial effects on observed phenomena, such as for example in machining (Sahin and Motorcu, 2004; Onwubolu, 2005; Lan, 2010).

The aim of this study is to describe the biphasic turbulent flow at the origin of erosion taking place inside the porous soil sample, considering the influence of wall roughness and variation of the concentration of clay in the flowing fluid.

MATERIALS AND METHODS

Two-dimensional modeling of the HET is achieved in this study through turbulence modeling by means of fluent software package. Fluent is a general purpose Computational Fluid Dynamics (CFD) code that has been applied to various problems in the fields of fluid mechanics and heat transfer. This code has been validated through numerous

investigations. Fluent is especially appropriate for the complex physics involved in heat and mass transfer and considers mixtures by modeling each fluid species independently or as a homogenized medium, (Escue and Cui, 2010; Vijapurapu and Cui, 2010).

There are many turbulence models available in Fluent. Use is made here of the ReNormalization Group (RNG) based k-ε turbulence model, (Yakhot and Orszag, 1986). Derivation of this model results in a model with constants different from those in the standard k-ε model and additional terms in the transport equations for the turbulent kinetic energy k and its rate of dissipation ε.

For the particular case of axisymmetric problems, the unsteady Reynolds averaged incompressible Navier-Stokes equations write:

$$\frac{1}{r} \frac{\partial(ru)}{\partial r} + \frac{\partial v}{\partial z} = 0 \quad (1)$$

$$\begin{aligned} \frac{\partial u}{\partial t} + \frac{1}{r} \frac{\partial(ru^2)}{\partial r} + \frac{\partial(uv)}{\partial z} = & -\frac{1}{\rho} \frac{\partial p}{\partial r} + \frac{1}{r} \frac{\partial}{\partial r} \left[r\mu \left(\frac{\partial u}{\partial r} - \overline{\rho(u')^2} \right) \right] \\ & + \mu \frac{u}{r^2} + \frac{\partial}{\partial z} \left[\mu \left(\frac{\partial u}{\partial z} - \overline{\rho u'v'} \right) \right] \end{aligned} \quad (2)$$

$$\begin{aligned} \frac{\partial v}{\partial t} + \frac{1}{r} \frac{\partial(ruv)}{\partial r} + \frac{\partial(v^2)}{\partial z} = & -\frac{1}{\rho} \frac{\partial p}{\partial z} + \frac{\partial}{\partial z} \\ & \left[\mu \left(\frac{\partial v}{\partial z} - \overline{\rho(v')^2} \right) \right] + \frac{1}{r} \frac{\partial}{\partial r} \left[r\mu \left(\frac{\partial v}{\partial r} - \overline{\rho u'v'} \right) \right] \end{aligned} \quad (3)$$

Where:

- t = The time
- ρ = The density of fluid
- u = The main velocity in the radial direction r
- v = The mean velocity in the axial direction z
- p = The pressure
- μ = The kinematics viscosity
- u' = The fluctuating component of radial velocity
- v' = The fluctuating component of axial velocity the symbol bar denotes statistical averaging

The special form of the transport equations RNG k-ε model contain the additional term R_ε. These equations write

$$\begin{aligned} \frac{\partial k}{\partial t} + \frac{1}{r} \frac{\partial(rku)}{\partial r} + \frac{\partial(kv)}{\partial z} = & \frac{1}{r} \frac{\partial}{\partial r} \left(\alpha\mu_r \frac{\partial k}{\partial r} \right) \\ & + \frac{\partial}{\partial z} \left(\alpha\mu_z \frac{\partial k}{\partial z} \right) + \alpha\mu_t \frac{k}{r^2} + \mu_t S^2 - \epsilon \end{aligned} \quad (4)$$

$$\begin{aligned} \frac{\partial \epsilon}{\partial t} + \frac{1}{r} \frac{\partial(r\epsilon u)}{\partial r} + \frac{\partial(\epsilon v)}{\partial z} = & \frac{1}{r} \frac{\partial}{\partial r} \left(\alpha\mu_r \frac{\partial \epsilon}{\partial r} \right) + \frac{\partial}{\partial z} \left(\alpha\mu_z \frac{\partial \epsilon}{\partial z} \right) \\ & + \alpha\mu_t \frac{k}{r^2} + C_{1\epsilon} \frac{\epsilon}{\rho k} - C_{2\epsilon} \frac{\epsilon^2}{\rho k} - \frac{1}{\rho} R_\epsilon \end{aligned} \quad (5)$$

With:

$$R_\epsilon = \frac{C_\mu \rho S^3 k^2 \epsilon (\eta_0 \epsilon - S\kappa)}{\eta_0 (\epsilon^3 + \beta S^3 k^3)}$$

and:

$$S = \sqrt{2 \left(\frac{\partial u}{\partial r} \right)^2 + 2 \left(\frac{\partial v}{\partial z} \right)^2 + \left(\frac{\partial v}{\partial r} + \frac{\partial u}{\partial z} \right)^2}$$

Where:

- α = The inverse effective Prandtl number for both k and ε
- C_{1ε} and C_{2ε} = Constants
- η₀ and β = Constants

The RNG k-ε model constants have values derived analytically by the RNG theory. They are given in Table 1. For further details, a complete description of RNG theory and its application to turbulence modeling can be found in (Choudhury, 1993; Pope, 2000).

Integration of the RNG-based k-ε turbulence model over the fluid domain enables calculation the wall shear τ. The classical linear erosion law predicts that erosion rate which corresponds to mass departure per unit time and by unit surface area is given by $\dot{\epsilon}_{er} = c_{er} (\tau - \tau_s)$ where c_{er} and τ_s are constant depending on the considering soil material. The rate $\dot{\epsilon}_{er}$ is related to time variation of local radius by $\dot{\epsilon}_{er} = \rho_d dR / dt$ where ρ_d is the dry density of soil. The erosion law yields that $\dot{\epsilon}_{er}$ is proportional to the amount of shear exceeding the shear threshold limit τ_s. The coefficient of proportionality c_{er} represents a measure of soil erodability under the action of a flowing fluid at the soil/fluid interface.

Under the assumption that the wall representing the soil/fluid interface is rigid and that the erosion law parameters remain constant, effects resulting from the applied hydraulic head, concentration of clay water content and roughness of the soil/fluid interface can be investigated through calculating the wall shear τ.

Simulation of the turbulent fluid flow taking place inside a cylindrical pipe having a rigid wall that replicates the geometry of the hole in the HET is considered in the following. The fluid domain is assumed to be axisymmetric. It extends 170 mm in the axial z-direction and 30 mm in the radial r-direction. The domain is oriented such that the inlet section is at left and the outlet section is at right.

Table 1: Values of constants of RNG k-ε model

C _μ	C _{ε1}	C _{ε2}	η ₀	β
0.085	1.42	1.62	4.38	0.012

The origin of the reference frame is placed at the entrance section. Figure 2 gives the geometry and the mesh of the tube with a detail zoom.

The wall at the top side of the fluid domain is assumed to be non uniform. Its geometry presents a roughness ϵ . This boundary of fluid domain is modeled here by a curved line assembled from 4 adjacent parabolas, Fig. 3. Each parabola extends over 1/4 length the hole. ϵ is defined as the total variation of the hole radius.

The boundary conditions that were used during simulation are the following:

- Inlet at the left extremity of the domain
- Outlet at the right extremity of the domain
- Symmetry type axis at the axis of symmetry which is the bottom side of the domain as presented in Fig. 2
- Wall at the top side of the domain

Roughness of the wall is considered to vary between 0.02 and 0.1 according to Table 2.

In addition to roughness, water clay content effect is modeled by considering various water-clay mixtures. The experimental values of density and dynamic viscosity at 20°C are given in Table 3 as function of the clay mass concentration.

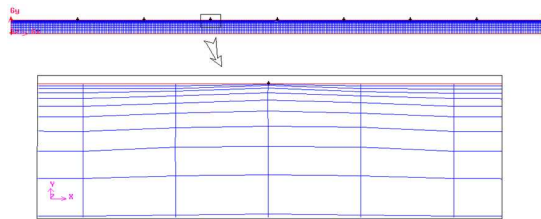


Fig. 2: Geometry and mesh of the tube

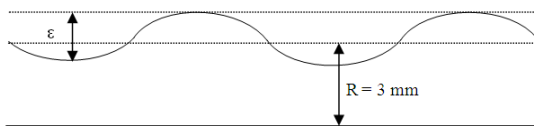


Fig. 3: The top side wall of the hole showing waviness aspect with roughness ϵ

Table 2: Values of roughness of the wall

Designation	(R1)	(R2)	(R3)	(R4)	(R5)
ϵ (mm)	0.02	0.04	0.06	0.08	0.1

Table 3: Homogenized density and viscosity for water-clay mixtures as function of clay concentration

Designation	Clay concentration (%)	Density of the mixture (kg m^{-3})	Viscosity of the mixture (pas)
C0	0.00	1000	0.00100
C1	3.85	1020	0.00194

RESULTS AND DISCUSSION

Three pressure gradients were applied. They correspond to $\Delta p = p_{\text{outlet}} - p_{\text{inlet}} = \rho g H$ where $g = 9.81 \text{ m sec}^{-2}$ and hydraulic head takes one of the following values: $H = 0.38 \text{ m}$, $H = 0.76 \text{ m}$ and $H = 1.14 \text{ m}$. Fixing $P_{\text{outlet}} = 0$, the inlet pressures are then: $P_{\text{inlet}} = 3726 \text{ Pa}$ (P1), $P_{\text{inlet}} = 7451 \text{ Pa}$ (P2) and $P_{\text{inlet}} = 11177 \text{ Pa}$ (P3).

Figure 4 and 5 give respectively, for clay concentrations C0 and C1, the wall-shear stress as function of the axial coordinate for the three applied hydraulic gradients and the five values of top wall roughness.

Figure 6 gives in the case concentration C1 static pressure at the axis of symmetry as function of the axial coordinate for the three applied hydraulic gradients and the five roughnesses.

Figure 7 gives, for the five roughnesses, pressure P2 and clay concentration C1, curves of the axial velocity at the axis of symmetry as function of the axial coordinate.

Table 4 gives the erosion rate (in $10^{-6} \text{ kg sec}^{-1}$). This amount is obtained by integrating the erosion law over the whole length of the hole and by multiplying the result by the initial circumference of the hole. The erosion constants used are: $c_{er} = 5.5 \times 10^{-4} \text{ s m}^{-1}$ and $\tau_s = 7 \text{ Pa}$. These correspond to a specific soil sample containing 50% kaolinit clay and 50% of sand that was tested.

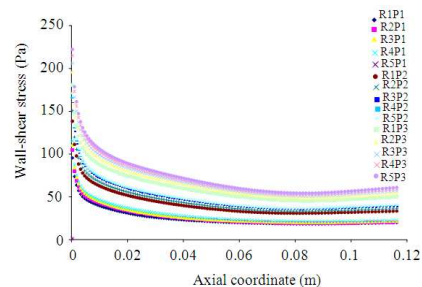


Fig. 4: Wall-shear stress obtained for the three pressures, the five roughnesses and C0

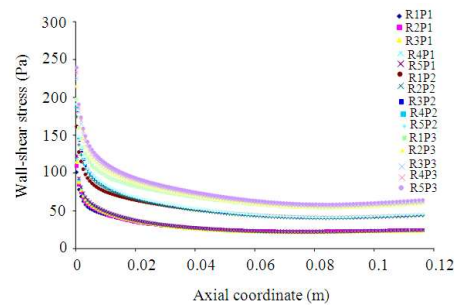


Fig. 5: Wall-shear stress as obtained for the three pressures, the five roughnesses and concentration C1

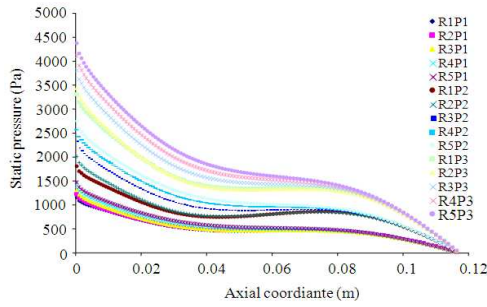


Fig. 6: Pressure at the axis of symmetry as function of the axial coordinate for concentration C1

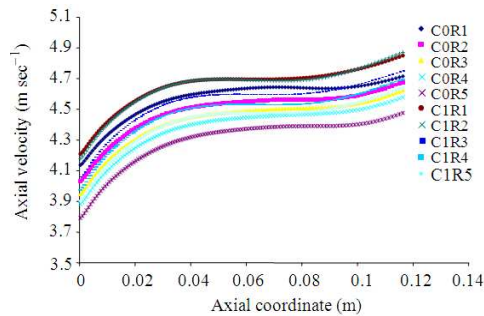


Fig. 7: Axial velocity at the axis of symmetry as function of the axial coordinate for pressure P3

Table 4: Erosion rate in 10⁻⁶ kg sec⁻¹ as function of inlet pressure and roughness for concentration C1

	R1	R2	R3	R4
P1	8.88	8.92	8.98	9.22
P2	17.98	18.15	18.54	18.88
P3	24.19	25.25	26.16	27.00

Table 4 presents, for concentration C1, the erosion rate as function of the various combinations associated to given hydraulic head and wall roughness.

Figure 4 and 5 show that the wall-shear is not uniform along the hole length. The wall-shear stress at the inlet extremity can exceed 7 times its permanent value in the plateau zone inside the hole. This is in true contrast with the habitual hypothesis used to derive one-dimensional modeling of the HET.

Figure 8 shows that the pressure gradient and wall roughness have remarkable effect on erosion rate. The erosion rate increases with increasing pressure head and roughness. In particular erosion rate at the outlet extremity of the hole is maximal. This enabled understanding why the eroded profile of the hole wall as observed during experiment is not uniform, Fig. 1.

Predicting erosion during the initial stage of piping formation can be done by the Fluent based model presented in this study. Flow features are however very complex in the real HET configuration.

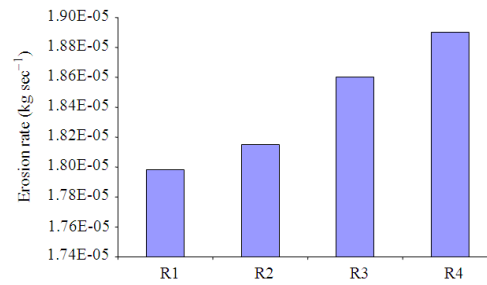


Fig. 8: Erosion rate as function of roughness for pressure P2 and concentration C1

In particular, clay concentration does not vary equally along the hole length, since it increases in the direction of flow with a maximum value occurring at the outlet extremity. The erosion law coefficients are also variable. Transport phenomenon of some soils particles that detach is also present. Further investigations including these aspects should be performed in order to get further insights in the complex physics of this simple experiment.

CONCLUSION

A two-dimensional modeling of the Hole Erosion Test was carried out in this study. This modeling considers the effect of roughness of the wall and of clay concentration on the development of erosion on the fluid/soil interface of the tube. Unlike the early models which are essentially one-dimensional, the two-dimensional modeling had shown that the wall-shear stress is not uniform along the hole wall. It was possible through using a linear erosion law to predict non uniform erosion along the hole length. Studying the effect of clay concentration and wall roughness has shown that their variations have considerable effect on the wall-shear stress and thus affect largely surface erosion that develops at the fluid soil sample interface.

ACKNOWLEDGEMENT

The authors would like to thank the Spanish Agency of International Cooperation which has supported financially this research under project grants: A/8816/07 and A/016344/08 as well as French CNRS and Moroccan CNRST under project grant: SPI02-08.

REFERENCES

Foster, M., R. Fell and M. Spannagle, 2000. The statistics of embankment dam failures and accidents. Can. Geotech. J., 37: 1000-1024. DOI: 10.1139/cgj-37-5-1000

- Bonelli, S. and O. Brivois, 2008. The scaling law in the hole erosion test with a constant pressure drop. *Int. J. Numer. Anal. Methods Geomech.*, 32: 1573-1595. DOI: 10.1002/nag.683
- Bonelli, S., O. Brivois, R. Borghi and N. Benahmed, 2006. On the modeling of piping erosion. *C.R. Mécanique*, 22: 555-559. DOI: 10.1016/j.crme.2006.07.003
- Choudhury, D., 1993. Introduction to the renormalization group method and turbulence modeling. Fluent Inc.
- Escue, A. and J. Cui, 2010. Comparison of turbulence models in simulating swirling pipe flows. *Applied Math. Model.*, 34: 2840-2849. DOI: 10.1016/j.apm.2009.12.018
- Fell, R., C.F., Wan, J. Cyganiewicz and M. Foster, 2003. Time for development of internal erosion and piping in embankment dams. *J. Geotech. Geoenviron. Eng.*, 129: 307-314. DOI: 10.1061/(ASCE)1090-0241(2003)129:4(307)
- Khamlichi, A., M. Bezzazi, L. El Bakkali, A. Jabbouri and B. Kissi *et al.*, 2009. Simplified analytical modeling of the normal test tube erosion. *Civil Eng.*, 155: 81-86. <http://dialnet.unirioja.es/servlet/articulo?codigo=3064296>
- Lan, T.S., 2010. Parametric deduction optimization for surface roughness. *Am. J. Applied Sci.*, 7: 1248-1253. DOI: 10.3844/2010.1248.1253
- Lachouette, D., F. Golay and S. Bonelli, 2008. One-dimensional modeling of piping flow erosion. *Comptes Rendus Mécanique*, 336: 731-736. DOI: 10.1016/j.crme.2008.06.007
- Onwubolu, G.C., 2005. A note on “surface roughness prediction model in machining of carbon steel by PVD coated cutting tools”. *Am. J. Applied Sci.*, 2: 1109-1112. DOI: 10.3844/2005.1109.1112
- Pope, S.B., 2000. *Turbulent Flows*. 1st Edn., Cambridge University Press, Cambridge, ISBN: 10: 0521598869, pp: 770.
- Richards, K.S. and K.R. Reddy, 2010. True triaxial piping test apparatus for evaluation of piping potential in earth structures. *Geotech. Test. J.*, 33: 20-33. DOI: 10.1520/GTJ102246
- Sahin, Y. and A.R. Motorcu, 2004. Surface roughness prediction model in machining of carbon steel by PVD coated cutting tools. *Am. J. Applied Sci.*, 1: 12-17. DOI: 10.3844/2004.12.17
- Vijiapurapu, S. and J. Cui, 2010. Performance of turbulence models for flows through rough pipes. *Applied Math. Model.*, 34: 1458-1466. DOI: 10.1016/j.apm.2009.08.029
- Wan, C.F. and R. Fell, 2004a. Investigation of rate of erosion of soils in embankment dams. *J. Geotech. Geoenviron. Eng.*, 30: 373-380. DOI: 10.1061/(ASCE)1090-0241(2004)130:4(373)
- Wan, C.F. and R. Fell, 2004b. Laboratory tests on the rate of piping erosion of soils in embankment dams. *Geotech. Test. J.*, 27: 1-9. DOI: 10.1520/GTJ11903
- Yakhot, V. and S.A. Orszag, 1986. Renormalization group analysis of turbulence: I-basic theory. *J. Sci. Comput.*, 1: 3-51. DOI: 10.1007/BF01061452